

## ELM-simulation experiments on Pilot-PSI using simultaneous high flux plasma and transient heat/particle source

G. De Temmerman<sup>1</sup>, J.J. Zielinski<sup>1</sup>, S. van Diepen<sup>1</sup>, H.J. van der Meiden<sup>1</sup>, L. Marot<sup>2</sup>, W. Melissen<sup>1</sup>, M. Price<sup>3</sup>, and J. Rapp<sup>1</sup>

1) FOM Institute for Plasma Physics Rijnhuizen, Association EURATOM-FOM, Trilateral Euregio Cluster, P.O. Box 1207, 3430 BE Nieuwegein, The Netherlands

2) Department of Physics, University of Basel, Klingelbergstrasse 82, CH-4056 Basel, Switzerland

3) EURATOM/CCFE Fusion Association, Culham Science Centre, Abingdon, UK

E-mail contact of main author: g.c.temmerman@rijnhuizen.nl

**Abstract.** Edge Localized Modes (ELMs) are a major concern for the lifetime of the divertor plasma-facing materials (PFMs) in ITER. The very high localized heat fluxes will lead to material erosion, melting and vaporization. In addition, the repetition of such thermal shocks can lead to a degradation of the material thermo-mechanical properties. In ITER, the PFMs will be submitted to both the steady state detached divertor plasma and the intense heat and particle fluxes during ELMs. In such a situation, the ELMs will interact with a surface modified by the intense fluxes of low energy ions, which are known to lead to strong modifications of the surface morphology. Moreover, the surface will be in equilibrium with the steady-state plasma and the near-surface will be loaded with helium and hydrogen isotopes. Such a situation might lead to strong synergistic effects which need to be investigated in details.

A new experimental setup is being developed at FOM Rijnhuizen for ELM simulation experiments with relevant steady-state plasma conditions and transient heat/particle source, allowing those effects to be studied in a self-consistent manner. The initial setup is based on the Pilot-PSI linear device and allows the superimposition of a transient heat/particle pulse to the steady-state heat flux plasma. Energy densities as high as  $1\text{MJ.m}^{-2}$  have been reached for a pulse duration of 1ms. In this contribution, we report on the first experiments were made to investigate the effect of the combined steady-state/pulsed plasma on polycrystalline tungsten targets. Post-mortem analysis of the targets was done by Scanning Electron Microscopy (SEM). Fast visible imaging was used to determine in-situ the threshold for tungsten release from the surface.

### 1. Introduction

Edge Localized Modes (ELMs) are a major concern for the lifetime of the divertor plasma-facing materials (PFMs) in ITER. The very high localized heat fluxes will lead to material erosion, melting and vaporization [1]. In addition, the repetition of such thermal shocks can lead to a degradation of the material thermo-mechanical properties. In ITER, the PFMs will be submitted to both the steady state detached divertor plasma and the intense heat and particle fluxes during ELMs. A steady-state heat flux of about  $10\text{MW.m}^{-2}$  is expected at the divertor targets while energy densities of up to  $10\text{MJ.m}^{-2}$  are predicted for natural ELMs [3]. Strong modifications of the surface morphology can occur during bombardment by low energy plasma ions (D,T, He) like blistering [4] or formation of helium-induced nano-structure [5]. In such a situation, the transient heat/particle pulse associated with an ELM will interact with a surface with modified properties which might strongly affect the material damage threshold [6,7].

Several techniques are currently being used to investigate the behaviour of materials under ITER relevant transient heat loads. Electron guns such as the JUDITH facility [8] can produce relevant energy densities and durations but lack the plasma environment. Plasma guns [9] on the other hand combine the plasma and heat loads relevant for the studies of ELM/material interactions but cannot combine it to the relevant steady-state plasma. Finally, the use of

powerful lasers associated with high flux linear plasma generators [5,7] combines a plasma environment and transient heat fluxes. Still, the plasma conditions in those devices are quite different from those expected in ITER and the use of a laser does not allow reproducing the transient particle flux associated with an ELM.

A new experimental setup is being developed at FOM Rijnhuizen for ELM simulation experiments with relevant steady-state plasma conditions and transient heat/particle source, allowing those effects to be studied in a self-consistent manner. The initial setup is based on the Pilot-PSI linear device and allows the superimposition of a transient heat/particle pulse to the steady-state heat flux plasma [10]. Energy densities as high as  $1\text{MJ}\cdot\text{m}^{-2}$  have been reached for a pulse duration of 1ms [11]. In this contribution, we report on the first experiments were made to investigate the effect of the combined steady-state/pulsed plasma on polycrystalline tungsten targets. Post-mortem analysis of the targets was done by Scanning Electron Microscopy (SEM). Fast visible imaging was used to determine in-situ the threshold for tungsten release from the surface.

## 2. Experimental

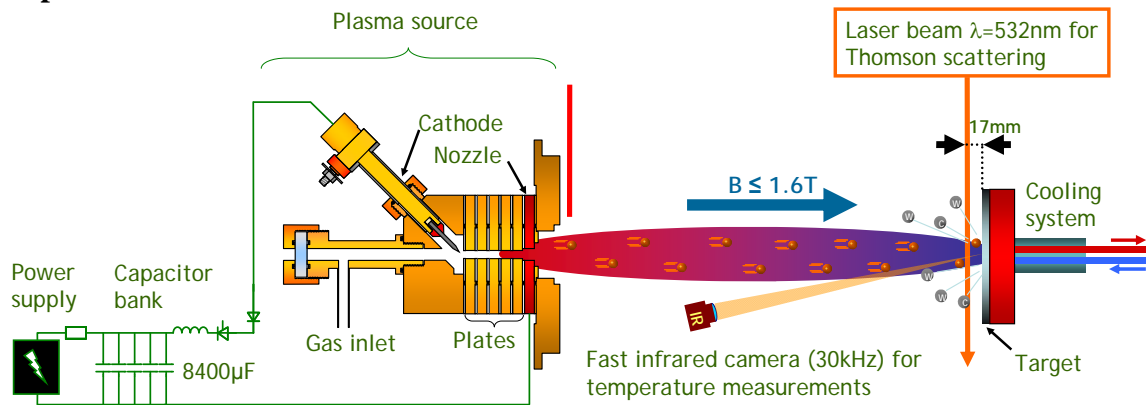


**Figure 1: Experimental setup of the pulsed plasma system in Pilot-PSI**

The Pilot-PSI linear device produces plasma parameters ( $n_e \sim 0.1\text{-}10 \times 10^{20}\text{m}^{-3}$ ,  $T_e \sim 0.2\text{-}5\text{eV}$ ) relevant to the study of steady-state plasma-surface interactions in the ITER divertor [12]. The cascaded arc plasma source is powered by a current regulated power supply. In parallel, a capacitor bank ( $8400\ \mu\text{F}$ ,  $4.2\ \text{kJ}$ ) is connected to the plasma source and discharged in the plasma source to transiently increase the input power (fig. 1). The pulse duration is about 1 ms. This results in the superimposition of a transient heat and particle pulse to the steady-state plasma. Peak discharge currents of about 11.6 kA have been generated, corresponding to a peak input power in the plasma source of about 4.5 MW. The evolution of the discharge current and voltage during a hydrogen plasma pulse is shown in fig.2. The steady-state current and voltage are 180V and 200A respectively, for a magnetic field of 1.6 T and a gas flow of 10 slm. Both the current and voltage in the source increase during the plasma pulse, although the voltage reaches a plateau after 0.5 ms. The peak input power in that case was about 3.8 MW. A short spike in the source voltage can be noticed at the beginning of the pulse, and lasts for about  $100\ \mu\text{s}$ . A more complete technical description of the system can be found in [10, 11]. The plasma source can be operated with a variety of gases (e.g. Ar, H, D, He, N) as well as with gas mixtures.

The plasma parameters are measured by means of a Thomson scattering system [9] located 17 mm in front of the target exposed to plasma beam (fig. 1). The magnetic field, the trigger to the capacitor bank and the Thomson scattering system were synchronized in time

with accuracy better than 1  $\mu\text{s}$  to ensure a reproducible time delay between every step of the sequence. The time evolution of the density and temperature during such a pulse have been described in [10].

The time evolution of the surface temperature during the pulse was monitored by a fast infrared camera (FLIR SC7500MB) which measures IR radiation in the wavelength range 2 -5  $\mu\text{m}$ . The frame rate of the camera was set to 10 kHz. The infrared camera I calibrated up to 3000 C using a blackbody source. Heat fluxes to the target are calculated with the THEODOR code [12], a 2D inverse heat transfer code. The heat fluxes derived by IR thermography have been compared to those calculated from the plasma density and temperature using sheath heat transmission factors and a relatively good agreement was found [10]. Fast visible imaging was done using a Photron APX-RS camera equipped with interference filters and operating at a framerate of 75 kHz.

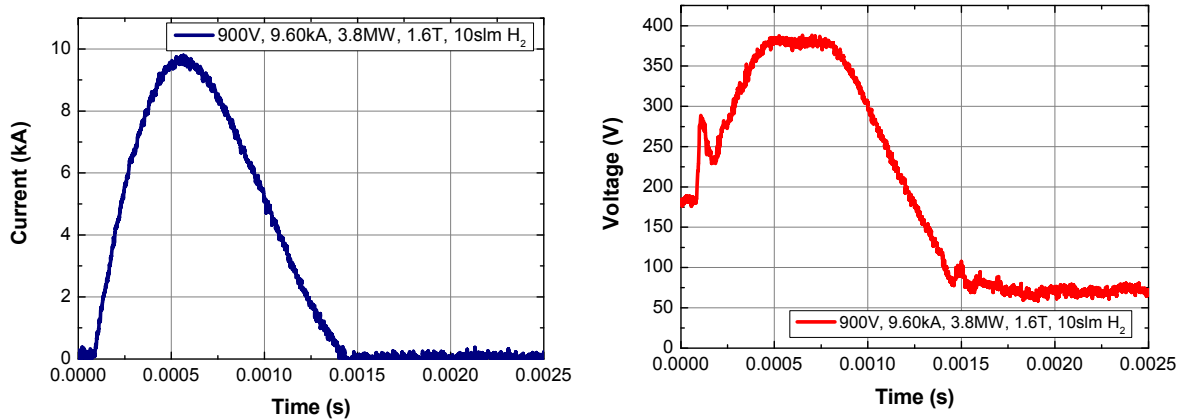


**Figure 2: Evolution of the discharge current and voltage during a hydrogen plasma pulse. The peak input power in the source is about 3.8MW.**

The plasma exposed target was a 30 mm diameter polycrystalline tungsten disc, 1mm thick, which was kept at floating potential during the exposure. After polishing, the targets are ultrasonically cleaned in ethanol and acetone. They are then outgassed at 1000C for 15 minutes following a temperature ramp of  $x\text{C}/\text{min}$ .

## 2. Properties of the pulsed plasma

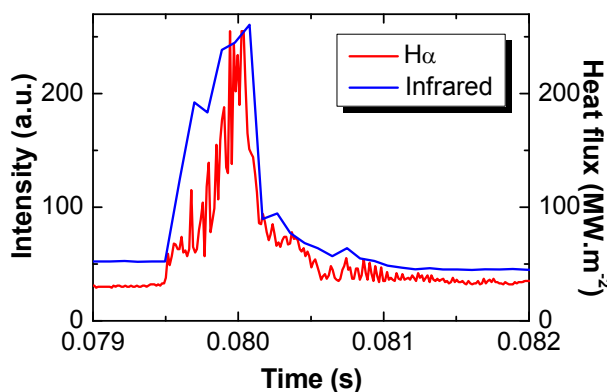


**Figure 3: Comparison of the time evolution of the  $H_{\alpha}$  line intensity and the power density to the target during a pulsed plasma**

Fig. 3 shows the time evolution of the  $H_{\alpha}$  signal measured by the fast visible camera during a pulsed plasma compared to the time evolution of the power flux density to the target determined from infrared thermography. The temperature rise time during a pulse is in the range 300-600 $\mu\text{s}$  which is in good agreement with typical risetimes for Type-I ELMs in tokamaks [3]. Evidently, the time evolution of the peak heat flux is well correlated with the time evolution of the  $H_{\alpha}$  signal, which in turn is well correlated with the time evolution of the discharge current [11].

The plasma parameters during a pulse

depend on the input power in the source, the magnetic field, source geometry and gas flow in the source. Fig.4 (a) illustrates the influence of the peak discharge current (i.e. the peak input power in the source) on the plasma density during the peak. The three different curves refer to different geometries of the plasma source. Both the diameter of the inside channel, and the geometry of the source nozzle were varied to find the best compromise between source performances and lifetime (details can be found in [11]). The plasma density increases with the discharge current, and the highest achieved plasma conditions are  $n_e=140\times 10^{20} \text{ m}^{-3}$  and  $T_e=6\text{eV}$ . The peak heat flux to the target naturally follows the same evolutions i.e. the higher the input power the higher the peak heat flux to the target (fig. 4b). A power scan has been done with hydrogen, helium and argon as working gas (fig. 4b), and similar heat load levels can be reached for the different gases.

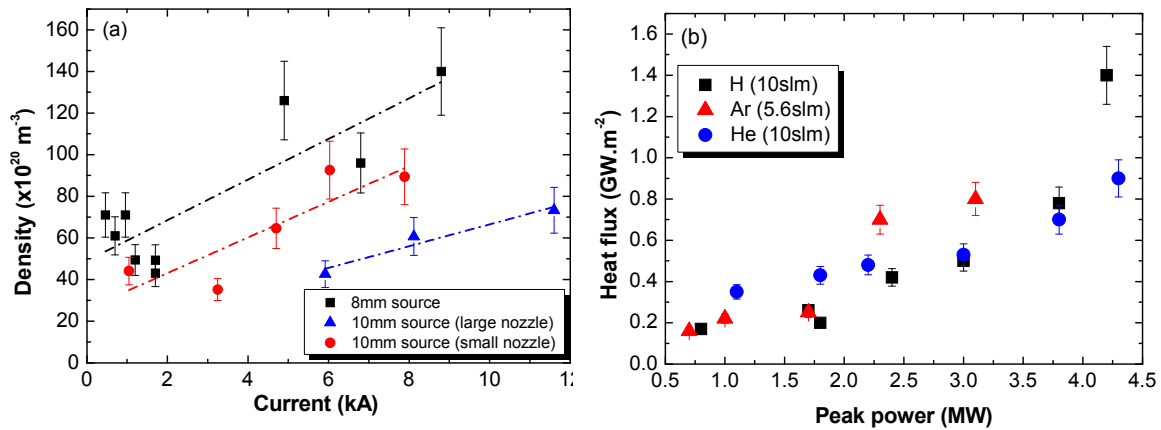


Figure 4: (a) Evolution of the peak plasma density for hydrogen pulses as a function of the discharge current in the source, and (b) evolution of the peak heat flux to the target as a function of the peak power in the source for different gases.

### 3. Behaviour of tungsten under simultaneous steady-state/pulsed plasma

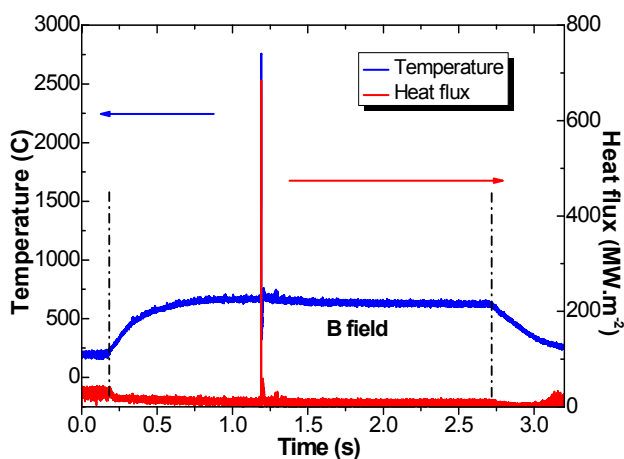
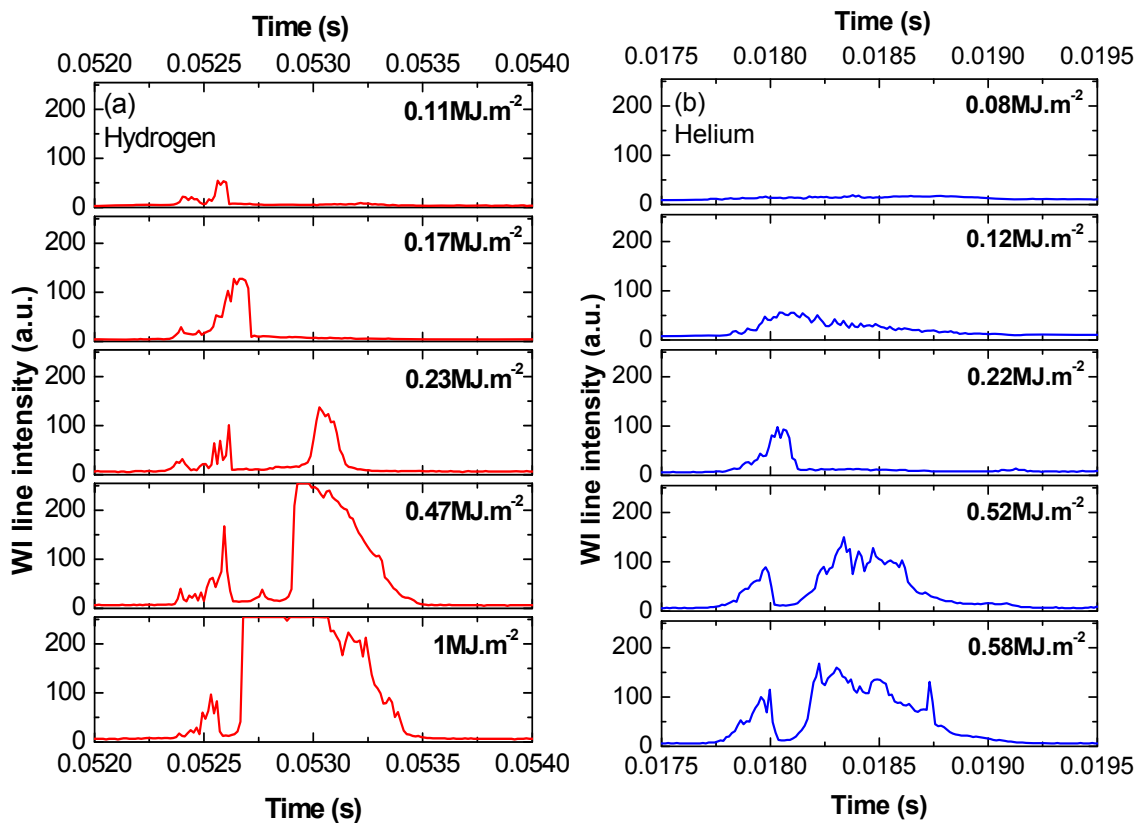


Figure 5: Temporal evolution of the surface temperature and heat flux, illustrating the superimposition of the steady-state and pulsed plasmas

Polycrystalline tungsten targets were exposed to combined steady-state/transient hydrogen and helium plasmas. The magnetic field is activated for 2s at 1.6 T and the capacitor bank is discharged into the plasma source at 1 s. Fig. 5 illustrates the evolution of the surface temperature during the experiment. The steady-state temperature is about 600 C and rises up to 2700 C during the plasma pulse. The magnetic field duration at 1.6 T is limited to 10s, and the repetition rate of the current capacitor bank is 4 discharges/min, so that only 1 pulse per discharge can be done at high fields. The plasma parameters in steady-state and during the pulse can be varied independently.

Two kinds of experiments were done. The same target was exposed to increasing energy densities and WI line emission at 400.9 nm was recorded by a fast visible camera, to characterize the damage threshold of tungsten. The steady-state discharge conditions were kept constant from shot to shot. The time evolution of the WI line intensity as a function of the energy density to the target is shown in fig. 6 for hydrogen and helium discharges. In both cases, the temporal evolution of the WI line can be divided into two phases. The first phase lasts for about 80-100  $\mu\text{s}$  at the beginning of the pulse and is present in most of the cases. From the sequences of snapshots shown in fig. 7, it is seen that this emission originates from the plasma source and is homogeneous along the plasma beam. Fig. 8 shows the time evolution of the WI signal at 2 different locations along the plasma beam respectively very close to the target (left of the images in fig. 5) and a few cm upstream (right side of the images in fig. 7). The first peak is observed at both locations with a slight time delay between both points consistent with travel along the plasma beam. After this first phase, there is a short period where the WI emission drops to almost zero. The subsequent phase is strongly dependent on the energy density deposited on the target. As seen from fig.7 and 8, the second emission peak for WI is only observed close to the target and does not propagate very far upstream. It is remarkable that the shape and duration of this first peak is similar to the initial voltage change inside the source during the plasma pulse. Since the cathode is made out of tungsten, it is not unreasonable to assume that this very rapid voltage change triggers an arc on the cathode releasing tungsten in the plasma which is then transported to the target.



**Figure 6: Time evolution of the WI line intensity close to the target for different energy densities during (a) hydrogen and (b) helium plasmas.**

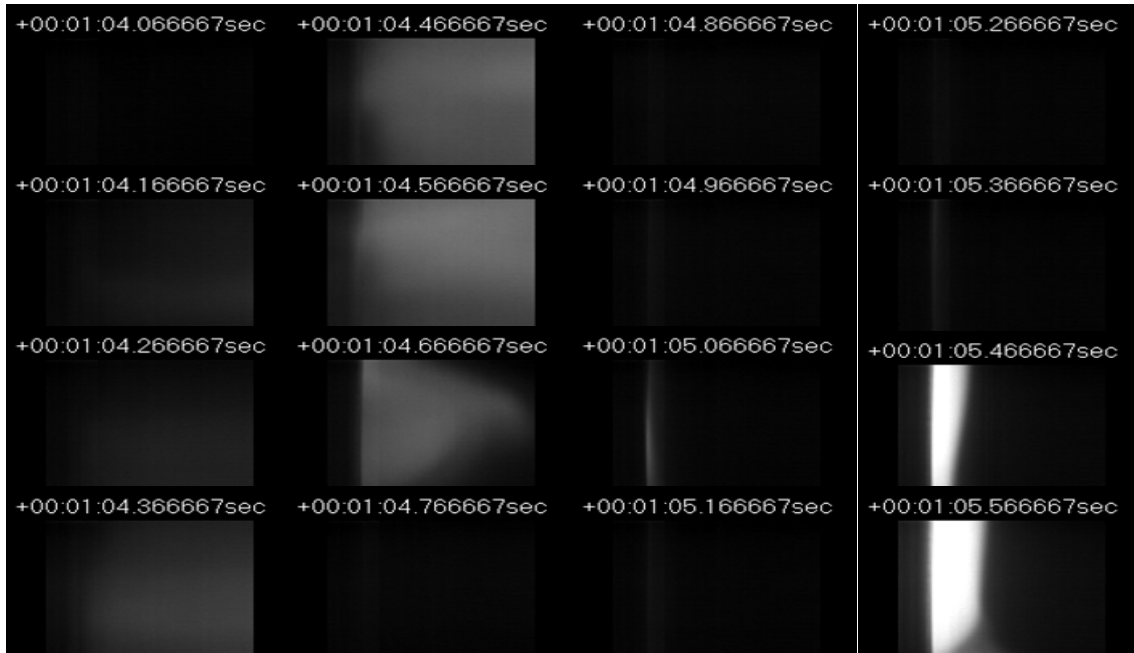


**Figure 7:** Series of snapshots measured by the fast filtered camera during a hydrogen plasma pulse with a deposited energy of  $0.47\text{MJ}\cdot\text{m}^{-2}$  (see fig. 5a). The first two columns correspond to the emission coming from the source followed by a quiescent period and then tungsten release from the target.

Tungsten release from the target shows a threshold effect, i.e. that no release is observed below a certain energy density while the line intensity increases with the deposited energy density after this threshold (fig. 6). The energy density threshold is found to be  $0.23\text{MJ}\cdot\text{m}^{-2}$  for hydrogen plasma+pulse (fig. 6a), while no release is observed below  $0.5\text{MJ}\cdot\text{m}^{-2}$  for helium plasmas (fig. 6b). The duration of the plasma-induced tungsten release also increases with the deposited energy density.

Although the melting temperature of tungsten is not expected to be affected by low energy ion irradiation, it was observed in [13] that the thermal shock resistance of tungsten was affected by the formation of helium-induced nanostructure on the surface.

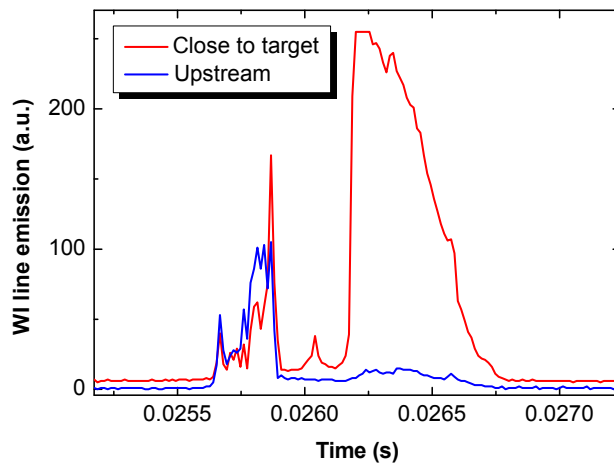


**Figure 8:** Time evolution of the WI line emission during a hydrogen plasma pulse with an energy density of  $0.47\text{MJ}\cdot\text{m}^{-2}$ , at 2 different locations from the plasma exposed target.

In that case, cracking of tungsten occurred at higher energy densities for targets pre-irradiated by low energy ions. In the present case, the exposure time is too low to lead to the creation of so-called tungsten ‘fuzz’ [13], although the surface morphology is strongly altered by the plasma exposure. The steady-state temperature of the target during the helium plasmas (around  $1500\text{C}$ ) is however high enough to allow the creation of helium holes and bubbles. In [6], the formation of helium-induced holes and bubbles

was found to decrease the ablation threshold of tungsten during simultaneous irradiation by helium plasma and nanosecond laser pulses. A lowering of the damage threshold of tungsten

was also observed for simultaneous hydrogen plasma and laser exposure in PISCES-A [7]. To our knowledge, no comparison of the damage threshold under similar hydrogen and helium conditions was made so far. More experiments are needed to understand the present results and assess the relationship between the surface morphology, the gas concentration in the near-surface region and the damage threshold under ELM-like conditions.

To investigate the effect of repeated simultaneous exposures to helium plasmas and transient heat/particle fluxes, a tungsten target was exposed to 10 sequences of 4s steady state helium plasmas with a plasma pulse in the middle of the sequence. The energy density during the plasma pulse was  $0.2 \text{ MJ.m}^{-2}$ , and the sample was kept at floating potential. After exposure, the samples were analyzed by Scanning Electron Microscopy (SEM) and Energy Dispersive X-Ray (EDX) analysis. The surface temperature in the centre of the plasma beam was about 1500 C. The peak temperature during the plasma pulse was about 2200 C.

In the area of highest heat and particle flux, circular holes are observed on the surface. Their diameter lies in the range 200-1000 nm. Interestingly, as shown in fig. 9b, protuberances can be observed on the walls of the holes, which in some ways look like blisters. The formation of holes and bubbles after low energy helium irradiation of tungsten has been well documented [5] and the present experimental conditions are well within the range of formation of such structures. It therefore appears that ELM-like heat/particle fluxes do not prevent the formation of He-induced nanostructure. Fig. 9c and d show the surface morphology of the same target 6mm away from the area of highest heat/particle flux. The morphology in that area is very different from that in the target middle. Sub-micrometer pinholes are observed throughout the observed areas. In addition, roughening of the surface is clearly seen. Here again, the surface morphology is very similar to that described in [5] which would indicate that the growth of helium-induced nano-structure is not affected by transient heat fluxes. It should be noted however, that more experiments are needed to document what would happen for higher ion fluences and larger number of transient events.

### ***Summary***

A new experimental setup has developed at FOM Rijnhuizen for ELM simulation experiments with relevant steady-state plasma conditions and transient heat/particle source, allowing plasma-surface interactions under those conditions to be studied in a self-consistent manner. The initial setup is based on the Pilot-PSI linear device and allows the superimposition of a transient heat/particle pulse to the steady-state heat flux plasma. Energy densities as high as  $1 \text{ MJ.m}^{-2}$  have been reached for a pulse duration of 1ms.

First experiments were made to investigate the effect of the combined steady-state/pulsed plasma on the morphology of polycrystalline tungsten targets. Post-mortem analysis of the targets was done by Scanning Electron Microscopy (SEM). Both hydrogen and helium plasmas were used. For helium plasmas, the transient heat/particle loads were found not to inhibit the formation of bubbles and pinholes on the surface. Cracking was observed for both helium and hydrogen plasmas. Tungsten release was observed by fast camera imaging (75kHz) to start at  $0.23 \text{ MJ.m}^{-2}$  for hydrogen plasma while no release is observed below  $0.5 \text{ MJ.m}^{-2}$  for helium plasmas.

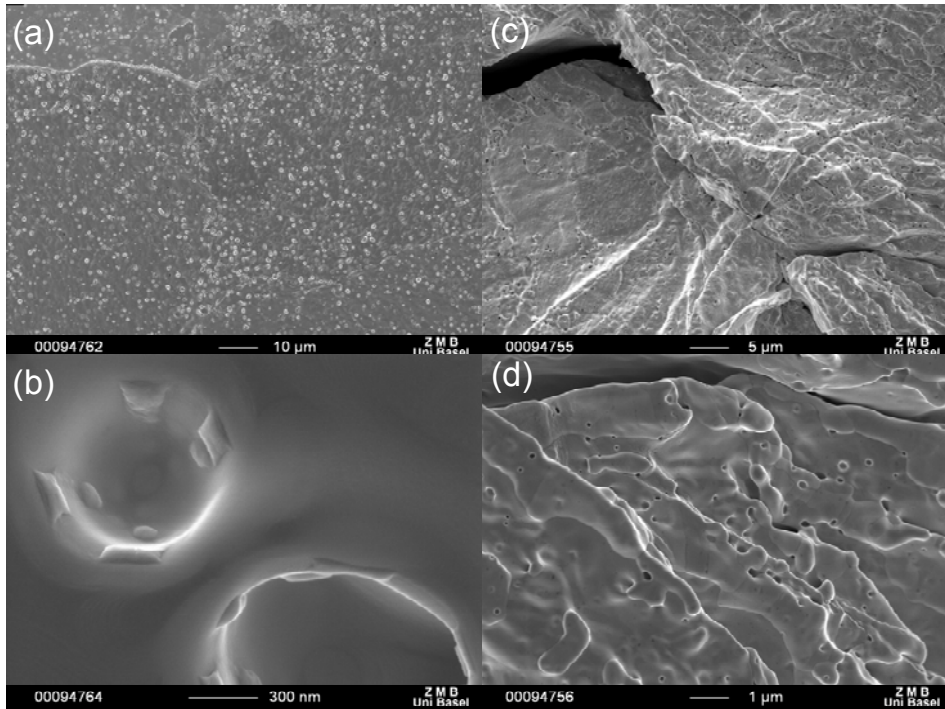


**Figure 9: SEM pictures showing the surface morphology of a polycrystalline tungsten target after exposure to 40s helium plasma and 10 plasma pulses with an energy density of  $0.2 \text{ MJ.m}^{-2}$ . Pictures (a) and (b) are taken in the target middle (highest heat fluxes) while fig. 9c and d are taken 6mm outwards.**

References:

- [1] N. Klimov, et al, J. Nucl. Mater., 390-391 (2009) 721
- [2] R.A. Pitts, et al, Phys. Scr., T138 (2000) 014001
- [3] A. Loarte, et al, Phys. Scr., T128 (2007) 222
- [4] K. Tokunaga, et al, J. Nucl. Mater., 337-339 (2005) 887
- [5] S. Kajita, et al, Nucl. Fusion 49 (2009) 095005
- [6] S. Kajita, et al, Appl. Phys. Lett., 91 (2007) 261501
- [7] K. Umstadter, R.P. Doerner, and G. Tynan, Phys. Scr., T 138 (2009) 014047
- [8] T. Hirai et al, Phys. Scr. T128 (2007) 166
- [9] I.E. Garkusha, et al, Phys. Scr., T138 (2009) 014054
- [10] G. De Temmerman, et al, Appl. Phys Lett., 97 (2010) 081502
- [11] J.J. Zielinski, et al, J. Nucl. Mater., in press
- [12] A. Herrmann, et al. Plasma Phys. Control. Fusion **37** (1995) 17
- [13] D. Nishijima, et al, J. Nucl Mater., in press.